Nanoscale

Dynamic Article Links

Cite this: *Nanoscale*, 2012, **4**, 5490

www.rsc.org/nanoscale

PAPER

Electronic structure and quantum transport properties of trilayers formed from graphene and boron nitride†

Xiaoliang Zhong,[a] Rodrigo G. Amorim,[a] Ralph H. Scheicher,[b] Ravindra Pandey*[a] and Shashi P. Karna[c]

Received 27th May 2012, Accepted 19th July 2012
DOI: 10.1039/c2nr31310c

We report the results of a theoretical study of graphene/BN/graphene and BN/graphene/BN trilayers using the van-der-Waals-corrected density functional theory in conjunction with the non-equilibrium Green's Function method. These trilayer systems formed from graphene and BN exhibit distinct stacking-dependent features in their ground state electronic structure and response to an applied electric field perpendicular to the trilayer planes. The graphene/BN/graphene system shows a negligible gap in the electronic band structure that increases for the AAA and ABA stackings under an external electric field, while the zero-field band gap of BN/graphene/BN remains unaffected by the electric field. When both types of trilayer systems are contacted with gold electrodes, a metal-like conduction is predicted in the low-field regime, which changes to a p-type conduction with an increase in the applied perpendicular bias field.

I. Introduction

Graphene has been a subject of extensive experimental and theoretical investigations due to its remarkable properties and novel potential applications.[1] For example, the electron mobility of graphene can reach as high as 10^5 cm^2 V^{-1} s^{-1} at room temperature, which is about 70 times higher than that of silicon.[2] This high electron mobility, combined with the ability to integrate well with other materials, makes graphene promising for high-frequency analogue electronics.[2] Its honeycomb lattice can be described in terms of a sp^2 hybridized network of carbon atoms. In its pristine form, the single-atom-thick layer 2D-graphene is a zero-gap semiconductor. Its electronic valence and conduction bands, which are associated with the π and π^* bands formed from C $2p_z$-orbitals, respectively, cross at Dirac points in the reciprocal space.[3] The absence of a band gap in graphene results from the equivalence of the two carbon sublattices. Thus it is possible to open a gap in the energy band by removing the sublattice equivalence, changing the electronic properties of graphene. In the recent years, several approaches, such as chemical doping,[4,5] edge functionalization,[6] change in the chemical composition of the substrate,[7–9] and application of external electric field[10] have been used to open a band gap in graphene for its potential usage in electronics. Positioning graphene in proximity to hexagonal boron nitride (h-BN), which has a lattice constant similar to graphene, but distinguishable sublattices consisting of boron and nitrogen atoms, can also introduce inequivalence in the graphene lattice and thus open a gap. In a recent theoretical study on graphene deposited on h-BN substrate,[9] a gap of 53 meV was predicted. The hybrid graphene/BN bilayer also shows band gap tunability in the presence of strain or an electric field.[11–14] Recent experiments[15,16] and theoretical studies[17] have shown that graphene deposited on bulk BN substrate behaves like free-suspended (zero-gap) graphene, which can be understood in terms of a competition between the induced *intraplanar* strains and the *interfacial* interactions in the graphene/bulk-BN system. For example, lattice constants of graphene and a BN monolayer match with each other in a bilayer superlattice,[18] whereas that in the case of graphene and bulk BN substrate[15–17] differ by about 1.6%. For the case of a bilayer graphene/BN superlattice, both graphene and BN compromise to match each other's lattice constant, forming the so-called 'commensurate' bilayer configuration, and the relatively small strain-induced energy penalty can be thoroughly compensated by the interlayer binding, leading to two globally *asymmetric* carbon sublattices of graphene.[18] Since the bilayer graphene/BN system is naturally asymmetric, with a finite band gap, it is natural to ask "what happens to the electronic structure and the band gap if one additional layer of BN or graphene is added?" In order to address this question, we have performed first-principles quantum chemical calculations on the electronic structure of trilayer, 'commensurate' superlattice configurations composed of graphene and BN.

Recently, several experiments[15,19–21] have reported deposition of graphene/BN hybrid systems. Liu *et al.*[19] have reported

[a]*Department of Physics, Michigan Technological University, Houghton, Michigan, 49931, USA. E-mail: pandey@mtu.edu*
[b]*Division of Materials Theory, Department of Physics and Astronomy, Uppsala University, Box 516, SE-751 20, Uppsala, Sweden*
[c]*US Army Research Laboratory, Weapons and Materials Research Directorate, ATTN: RDL-WM, Aberdeen Proving Ground, MD 21005-5069, USA*

† Electronic supplementary information (ESI) available. See DOI: 10.1039/c2nr31310c

chemical vapor deposition (CVD) of h-BN on graphene. The fabricated graphene-BN films have thicknesses of about two to a few monolayers. Very recently, Britnell *et al.*[21] reported the fabrication of a graphene-based device in which up to 30 layers of h-BN were sandwiched between two graphene monolayers. Such vertical graphene heterostructures were shown to act as an effective field-effect tunneling transistor with a room-temperature switching ratio of about 50 (ref. 21). Theoretical calculations have shown the dependence of the band gap on the number of h-BN layers in a bilayer-graphene/several-layer BN system.[22]

Trilayer graphene and BN/graphene/BN systems have also been the subject of several recent studies. The trilayer graphene system exhibits stacking-dependent electronic properties under the influence of a perpendicular electric field, with the semiconducting ABC stacked trilayer showing a large tunable gap relative to the metallic ABA stacked trilayer.[23–27] While monolayer graphene keeps its gapless feature in the presence of a perpendicular electric field, a BN/graphene/BN trilayer system shows stacking-dependent energy gap tunability.[13,28,29]

In this study, we consider a graphene/BN/graphene trilayer system to investigate the effect of an inserted layer of BN on the electronic properties of the bilayer graphene with and without perpendicular external electric field. We find that the graphene/BN/graphene trilayer exhibits a negligible energy gap regardless of the stacking configurations considered. However, this hybrid trilayer system exhibits interesting stacking-dependent gap tunability under the application of a perpendicular external electric field.

Using van der Waals force corrected-density functional theory (vdW-DFT), we performed calculations on trilayers composed of graphene and BN to predict their stacking-dependent stability, electronic structure, and electron transport properties under an applied external perpendicular electric field. In addition, we also performed electron transport calculations on BN/graphene/BN trilayer.

The rest of the paper is organized as follows: Section 2 gives the details of the computational methods. Results are discussed in Section 3 and a summary is given in Section 4.

II. Methods and computational details

In the present vdW-DFT approach, the exchange correlation functional form includes the non-local part of the dispersion correlation and is not a semi-empirical addition to the DFT Hamiltonian.[30,31] Briefly, the vdW energies arising from electron–electron correlation are incorporated into the total exchange-correlation energy as follows:

$$E_{xc}[n(\boldsymbol{r})] = E_x^{GGA}[n(\boldsymbol{r})] + E_c^{LDA}[n(\boldsymbol{r})] + E_c^{nl}[n(\boldsymbol{r})] \quad (1)$$

where the $E_x^{GGA}[n(\boldsymbol{r})]$ is the exchange energy described through the semi-local generalized gradient approximation (GGA), $E_c^{LDA}[n(\boldsymbol{r})]$ is the local part of correlation energy described in the local density approximation (LDA) and $E_c^{nl}[n(\boldsymbol{r})]$ is the non-local part of correlation energy given by

$$E_c^{nl}\left[n(r)\right] = \frac{1}{2}\iint \mathrm{d}^3 r_1 \mathrm{d}^3 r_2 n(r_1) n(r_2)(q_1, q_2, r_{12}) \quad (2)$$

where $r_{12} = |\boldsymbol{r}_1 - \boldsymbol{r}_2|$, and q_1, q_2 are the values of a universal function $q_0[n(\boldsymbol{r}),|\nabla n(\boldsymbol{r})|]$, evaluated at $\boldsymbol{r}_1$ and $\boldsymbol{r}_2$. The kernel also has a universal form satisfying (i) E_c^{nl} is strictly zero for any system with constant density; and (ii) the interaction between any two molecules has the correct r^{-6} dependence for large separations.[30–32] It is to be noted that the vdW functional form implemented in the SIESTA program package has been successfully applied to systems such as pairs of atoms and molecules, molecules adsorbed on surfaces, molecular solids, and biological systems.[33] For example, in a semiconducting crystal consisting of carbon nanotubes (CNTs), the vdW-DFT approach predicts the wall-to-wall separation to be 3.45 Å, in excellent agreement with the corresponding experimental value of 3.4 Å.[34]

Norm-conserving pseudopotentials[35] and double-zeta basis sets with polarization orbitals were used for all atoms in electronic structure calculations. All calculated equilibrium configurations were fully relaxed, with residual forces smaller than 0.01 eV Å^{-1}. The reciprocal space integration to optimize the geometrical configuration was initially performed with a grid of $30 \times 30 \times 1$ k-points. Total energy, band structure and density of states of the optimized configurations were then calculated with a grid of $100 \times 100 \times 1$ k-points.

Our trilayers represent commensurate in-plane structures which are analogous to the so-called strained-layer semiconducting superlattices. The lattice constant along the direction perpendicular to the graphene plane is taken to be 30 Å, and the common lattice constant of the sandwich structure is fully optimized yielding a marginally small isotropic strain in both graphene and BN. Note that the difference in the lattice constants of graphene and BN is about 1.6%, and graphene is always gapless under isotropic strain.[36] This is not the case with uniaxial strain, where one needs to be careful in the determination of points of high symmetry in the reciprocal space since the position of the K point in the high symmetry of the graphene Brillouin zone is misplaced.[37,38]

The zero-bias conductance, bias-dependent electron transmission and current were calculated using the non-equilibrium Green's function (NEGF) method based on the Keldysh formalism, as implemented in the Transiesta program package.[39] The current through the gold-connected hybrid multilayer system can be obtained as

$$I = \frac{e}{h}\int_{-\infty}^{\infty} \mathrm{d}E\, T(E,V)\left[f(E-\mu_1) - f(E-\mu_2)\right] \quad (3)$$

where μ_1 and μ_2 are the electrochemical potentials in the two gold contacts under an external bias V, $f(E)$ is the Fermi–Dirac distribution function. The transmission function, $T(E,V)$, is an important intrinsic factor describing the quantum mechanical transmission probabilities for electrons. The semi-infinite effect of the left (right) electrode is taken into account by introducing the self-energy Σ_L (Σ_R) in the effective Hamiltonian. It is worth noting that the transmission depends on both the electron energy E and the applied external bias V.

For the metal contacts, Au atoms were used in the transport calculations. For Au atoms, pseudopotentials augmented by 5d and 6s functions reproduced the electronic properties of bulk Au near the Fermi region. This Au basis set has been used in previous electron transport studies on Au–C_{60}–Au (ref. 40) and Au–graphene–Au systems.[41]

A grid of 16 × 16 k-points, perpendicular to the transport direction was used. The distance between gold and the nearest monolayer was taken to be 2.1 Å, though the equilibrium binding distance of graphene[42–44] and BN[45] on Au(111) has been reported to be between 3 and 3.5 Å. We also performed electron transport calculations using Au and graphene (BN) distance of 3.5 Å. The results for the transmission function and the I–V characteristics were very similar to the ones calculated at the distance of 2.1 Å, though a slightly smaller magnitude of the current at a given applied bias voltage is calculated at the larger contact-trilayer separation.

III. Results and discussion

For the geometry and electronic structure calculations, we used van der Waals (vdW) corrected density functional theory (DFT) method implemented in the SIESTA electronic structure program package.[30,31] In previous studies,[12,41,46,47] the local density approximation (LDA)-DFT method has been found to be satisfactory in reproducing interlayer spacings in graphitic systems. However, LDA tends to underestimate the interlayer binding energies[48] compared with experiments[49,50] due to its localized nature. The inclusion of a vdW term representing dispersive forces in the electronic Hamiltonian becomes essential in obtaining accurate predictions in geometry and in particular energetics for graphene-based materials.[17,43,51–54] For example, the calculated binding energy per atom for graphite is 17 meV at the LDA-DFT level of theory, while inclusion of the vdW term yields a binding energy per atom of 45 meV, in excellent agreement with experiment.[49,50] When graphene is deposited on top of a BN substrate, the interface bonding is exclusively due to long-range van der Waals forces.[17] The vdW-DFT method has also been found to provide accurate descriptions of geometrical and electronic structures, binding energy, and electron tunneling between metallic surfaces, including graphene.[43,51–53] Absence of vdW corrections has been shown to lead to significant overestimation of the structural corrugation in the Moiré pattern.[51]

Structural properties

A trilayer consisting of graphene and BN has more stacking possibilities than those in a graphene/BN bilayer, since each adjacent bilayer can be stacked in three distinct arrangements.[12] Here we restrict ourselves to investigate only three trilayer stacking arrangements, namely AAA (hexagonal), ABA (Bernal) and ABC (rhombohedral), which may be considered as the most typical configurations.[29] The ABA stacked trilayer is taken to be composed of the AB (boron) bilayer configuration which was predicted to be the most stable stacking arrangement for a graphene/BN bilayer at the vdW-DFT level of theory. In the AB (boron) bilayer configuration, the boron sublattice of one layer is on top of one carbon sublattice of the other layer, while the nitrogen sublattice is on top of the center of one hexagonal carbon ring.[12] The vdW-DFT interlayer spacing for AB (boron) configuration of the graphene/BN bilayer found by us is 3.32 Å and is in agreement with the value of 3.35 Å obtained from calculations using the random-phase approximation to the correlation energy.[17]

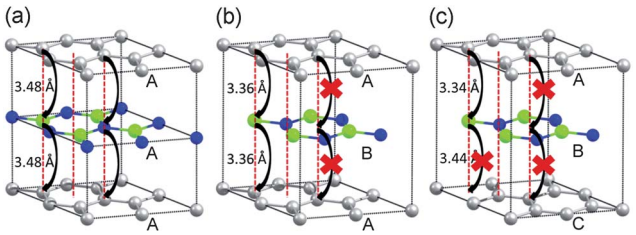

Fig. 1 A schematic diagram of the stacking arrangements considered for graphene/BN/graphene. The AAA, ABA and ABC stackings are represented in (a)–(c), respectively. The gray, green, and blue spheres represent carbon, boron, and nitrogen atoms, respectively. The black curved arrows show the possible atomic coupling between adjacent layers, while the red crosses indicate the couplings which in practice are not available.

Fig. 1 shows the stacking arrangements considered for the graphene/BN/graphene trilayer. In the AAA stacking (Fig. 1(a)), all three constituent layers project themselves to the same image on a plane parallel to them, *i.e.*, each adjacent layer pair is AA stacked. In the ABA stacking (Fig. 1(b)), the two graphene layers have the same projection on this plane and the BN layer is AB (boron) stacked to both graphene layers. Finally, the ABC stacking (Fig. 1(c)) represents the case where all three layers have different projections on this plane. While the BN layer is AB (boron) stacked to the upper graphene layer, it is AB (nitrogen) stacked to the lower graphene layer.

Table 1 gives the calculated values of binding energy, intraplanar bond length (R), intraplanar lattice constant (a) and interplanar spacing (Z) for various graphene/BN/graphene and BN/graphene/BN trilayer stacking configurations. Note that all three constituent layers in one trilayer system match their in-plane lattice constants with each other, forming the so-called 'commensurate' configuration. The binding energy is defined as the difference in total energy of an assembled trilayer system and that of the corresponding individual total energies of the isolated constituent monolayers, and is normalized to formula unit.

The ABA stacking arrangement for graphene/BN/graphene is predicted to be the most stable configuration with R of 1.451 Å and Z of 3.36 Å. Note that the calculated R of graphene and a BN monolayer are 1.448 and 1.459 Å, respectively. The calculated R of graphene/BN/graphene is a weighted mean of the bond lengths of the constituent layers, and is independent of the stacking arrangements (Table 1). On the other hand, the calculated Z of graphene/BN/graphene (~3.36 Å) gets modified slightly relative to that in the constituent bilayers (~3.32 Å). Z also depends on the stacking arrangements following the order of $Z_{AAA} > Z_{ABC} > Z_{ABA}$ which is directly related to the order of $Z_{AA} > Z_{AB\ (nitrogen)} > Z_{AB\ (boron)}$ calculated for graphene/BN bilayer at the vdW-DFT level of theory.[55]

A higher value of the binding energy of the ABA trilayer can be traced back to the constituent graphene/BN bilayer. The calculated results show that the resultant binding of a graphene/BN bilayer is a delicate balance between short-range Pauli's repulsive forces and long-range vdW attractive forces. For the equilibrium separation of the AB-stacked system, the magnitude of the Pauli's repulsive forces is larger in the AA-stacked system relative to that of the AB-system. As a result, the equilibrium spacing for the AA stacked bilayer is always higher than that of

Table 1 Structural properties of graphene/BN/graphene and BN/graphene/BN at the vdW-DFT level of theory

System	Stacking configuration	Binding energy/formula unit (eV)	(Intraplanar) bond length R (Å)	(Intraplanar) lattice constant a (Å)	Interplanar spacing Z (Å)
Graphene/BN/graphene	AAA	0.254	1.451	2.513	3.48
Graphene/BN/graphene	ABA	0.289	1.451	2.513	3.36
Graphene/BN/graphene	ABC	0.283	1.451	2.513	3.34, 3.44
BN/graphene/BN	AAA	0.241	1.454	2.518	3.52
BN/graphene/BN	ABA	0.273	1.455	2.520	3.37
BN/graphene/BN	ABC	0.274	1.455	2.520	3.38

AB stacked bilayer leading to a smaller binding energy for the AA-stacked system (see ESI, Fig. S1†).

Comparison of our results with the ABA-stacked trilayer graphene (see ESI, Fig. S2†) suggests that the substitution of a central graphene with a BN monolayer modifies Z from 3.42 to 3.36 Å at the vdW-DFT level of theory. The calculated binding energy values are 0.289 and 0.255 eV for the ABA-stacked graphene/BN/graphene and trilayer graphene, respectively. This difference can be attributed to dissimilarity of the constituent layers, though the layers are stacked in a same order. The constituent bilayers (*i.e.* graphene/BN and graphene/graphene) have similar long-range vdW attractive forces acting on each-other at larger interlayer distances, whereas the short-range Pauli's repulsive forces acting on the graphene/graphene bilayer is larger than that of graphene/BN bilayer due to differences in the effective atomic volume of C in graphene and B and N in the BN lattice [ref. 56, see ESI, Fig. S3†].

Fig. 2 shows the stacking arrangements considered for BN/graphene/BN. The ABA and ABC stacked configurations are predicted to be nearly degenerate (Table 1) at the vdW-DFT level of theory. The calculated R and Z for BN/graphene/BN also follow their respective values in the constituent bilayers. For example, R is independent of the stacking arrangements, and is about the weighted mean of constituent monolayers. The ABA and ABC stacked configurations are both composed of two AB (boron) bilayers with the same interplanar spacing of 3.37 Å (Table 1), whereas Z of the AAA-stacked BN/graphene/BN trilayer is calculated to be 3.52 Å. A previous LDA-DFT study has predicted the ABA and ABC stacking configurations to be degenerate with the same Z of 3.22 Å.[28]

Electronic properties

The electronic band structure along the high symmetry points in k-space of the energetically preferred ABA-stacked configurations of graphene/BN/graphene and BN/graphene/BN are plotted in Fig. 3. We note that the band structure of a graphene/BN bilayer near Fermi energy is dominated by C-p_z orbitals. The calculated energy gap at K is 43 meV at the vdW-DFT level of theory which is mainly due to the interaction of graphene with the BN monolayer where two sublattices in graphene experience a slightly different electrostatic potential due to inhomogeneous charge distribution present in the heterogeneous BN monolayer.[12]

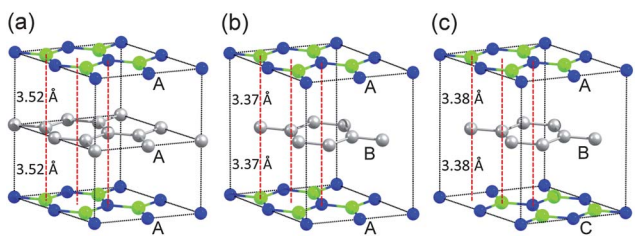

Fig. 2 A schematic diagram of the stacking arrangements considered for BN/graphene/BN. The AAA, ABA and ABC stackings are represented in (a)–(c), respectively. The gray, green, and blue spheres represent carbon, boron, and nitrogen atoms, respectively.

In the ABA-stacked graphene/BN/graphene trilayer, the graphene layers are structurally symmetric. Although the interaction between top and bottom graphene layers with the central BN monolayer lifts the degeneracy of bands associated with graphene near the Fermi energy (Fig. 3(b)), the overall symmetry between the top and bottom graphene layers yields a negligible energy gap. The calculated projected density of states (PDOS) and local density of states (LDOS) show that the low energy bands near Fermi energy solely originate from graphene layers (see ESI, Fig. S4 and S5†). No shift of the Dirac point away from the high symmetry K point in the reciprocal space is predicted. The calculated band gap remains nearly zero ($\approx$1 meV) for the ABA-stacked graphene/BN/graphene. This is also the case with the AAA and ABC-stacked trilayers where the gap is calculated to be 4 and 6 meV, respectively. Note that trilayer graphene in AAA, ABA, and ABC-stacked configurations all have a zero gap at the vdW-DFT level of theory.[55]

For the case of BN/graphene/BN trilayer, the band gap appears to be relatively more sensitive to the stacking arrangements. The band gap for AAA, ABA and ABC stacking arrangements are calculated to be 116, 57 and 5 meV, respectively at the vdW-DFT level of theory. The difference in band gap values can be understood by a straightforward analysis. In AAA stacking, while one carbon sublattice is coupled with boron sublattices in both BN layers, the other carbon sublattice is coupled with nitrogen sublattices. The high asymmetry in electronegativity between boron and nitrogen sublattices induces a significant corresponding asymmetry in the two carbon sublattices of the central graphene layer. In ABA stacking, while one carbon sublattice (sublattice I) is coupled with two boron sublattices, the other carbon sublattice (sublattice II) is in between the centers of BN hexagonal rings (Fig. 2(c)). Compared with AAA stacking, in ABA stacking the asymmetry in two carbon sublattices induced by the difference between boron and nitrogen is lower because carbon sublattice II is relatively far from both boron and nitrogen. On the other hand, top and bottom BN layers in the ABC-stacked configuration do not induce an asymmetry between two carbon sublattices of the central layer (Fig. 2(c)), leading to a tiny band gap of 5 meV, as also predicted

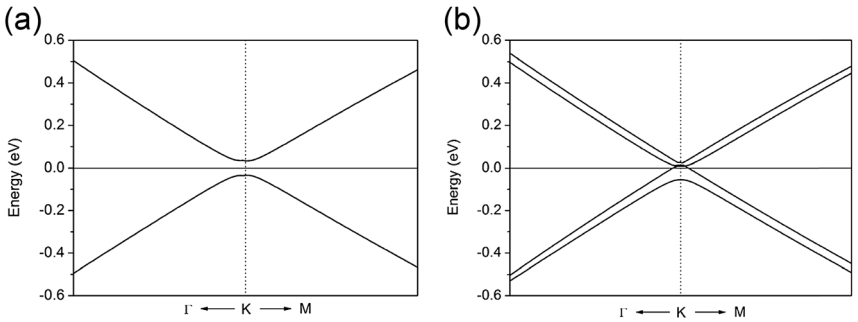

Fig. 3 The calculated band structures of (a) ABA-stacked BN/graphene/BN and (b) ABA-stacked graphene/BN/graphene. Zero of the energy is aligned to the Fermi level.

by previous calculations.[13] As a consequence, AAA shows the highest energy gap, followed by ABA, while ABC stacking exhibits a virtually negligible gap.

Effect of electric field on band structure

Fig. 4 shows a variation of the minimum energy gap under the influence of the electric field applied perpendicularly to the layered configurations. The direction of applied field is from bottom layer to top layer, and we restrict ourselves to electric field strengths below 1 V nm^{-1}, considering that the breakdown field of BN sheets is reported to be 0.7 V nm^{-1}.[15] It is to be noted here that the AAA and ABA stacked graphene/BN/graphene (BN/graphene/BN) configurations exhibit mirror symmetry about the central layer, and the ABC stacked BN/graphene/BN trilayer exhibits point symmetry about the midpoint of two (left most) carbon atoms shown in Fig. 2(c). Thus, no changes in the electronic properties are expected when the direction of electric field is reversed for these trilayers. On the other hand, the ABC stacked graphene/BN/graphene trilayer has neither mirror symmetry nor point symmetry. However, reversal of the electric field is expected to have a minimal effect due a lack of effective interaction between top and bottom graphene layers, as will be shown below.

A distinct behavior in electronic properties is exhibited by the graphene/BN/graphene and BN/graphene/BN trilayers in the presence of the perpendicular external field; the former configuration shows a significant modulation of band gap whereas the latter configuration does not show any modulation in its band gap (Fig. 4(a)). This difference is consistent with the previously reported LDA-DFT calculations.[13]

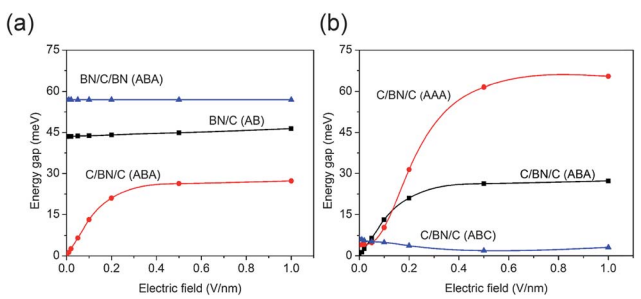

Fig. 4 The minimum energy gap as a function of perpendicular electric field: (a) ABA-stacked BN/graphene/BN, ABA-stacked graphene/BN/graphene and AB-stacked BN/graphene, (b) AAA-, ABA- and ABC-stacked graphene/BN/graphene.

For the ABA-stacked BN/graphene/BN trilayer, we find an invariable band gap of 57 meV with the applied electric field up to 1 V nm^{-1}. On the other hand, the ABA-stacked graphene/BN/graphene trilayer shows gap tunability with the applied electric field up to 0.5 V nm^{-1}, where the gap saturates at about 27 meV, showing virtually no further changes with increasing electric field up to 1 V nm^{-1}. Thus, graphene/BN/graphene behaves more like a graphene bilayer, but with a weaker and indirect (*via* BN layer) graphene–graphene interaction and a less tunable band gap. For the graphene bilayer, we found a nearly linear relationship between the energy gap and the magnitude of an external electric field ranging from 0 to 1 V nm^{-1} at the vdW-DFT level of theory,[55] in excellent agreement with experimental results.[57] Also, our vdW-DFT results for graphene/BN bilayer[55] are in agreement with the previous theoretical study showing a much weaker, but linear response of the energy gap to the external electric field.[11]

As shown in Fig. 4(b), the stacking arrangements in the graphene/BN/graphene trilayer appear to play a major role on the field tunability of the band gap. Both the AAA and ABA stacking configurations show significant gap variation with the applied electric field, whereas the ABC stacked configuration shows little change (even a small reduction) in the energy gap with increasing applied perpendicular electric field (Fig. 4(b)). This is in sharp contrast to the behavior found in a graphene trilayer, where the ABC stacking configuration exhibits larger band gap modulation than the AAA or ABA stacking configurations.[24]

A band gap in the hybrid graphene/BN bilayer in the presence of an external field applied perpendicularly is attributed to the different electrostatic potential experienced by the carbon sublattices in graphene due to the inhomogeneous charge distribution present in BN.[11,12] Thus, the stacking sequence which would facilitate a larger interlayer coupling to introduce high asymmetry in the sublattices of graphene is likely to lead to a significant energy dispersion of electronic bands near the Fermi surface. For graphene/BN/graphene, topology of the AAA stacking facilitates an overlap of p_z orbitals of adjacent graphene and BN layers, since all carbon atoms in graphene and all boron and nitrogen atoms in BN are placed at the same in-plane atomic positions (*i.e.*, on top of each other). This is not the case with the ABA-stacked trilayer system where one of the carbon sublattices

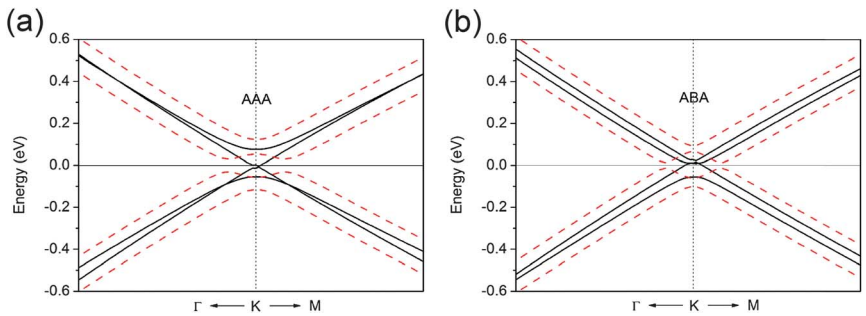

Fig. 5 Electronic band structures of (a) AAA- and (b) ABA-stacked graphene/BN/graphene trilayers. Solid black: field = 0. Dashed red: field = 0.5 V nm^{-1}. Zero of the energy is aligned to the Fermi level.

is just on top of the center of h-BN hexagonal ring. Likewise, the degree of the asymmetry induced by the adjacent BN layer on the carbon sublattices for the AAA-stacked trilayer is significantly larger than that for the ABA-stacked trilayer which in turn leads to a larger tunability of its energy gap in the presence of an electric field.

Considering that no asymmetry in the carbon sublattices is induced by the central BN lattice for the graphene/BN/graphene trilayer system, both top and bottom graphene layers prefer the AA-stacking format. Unlike the AB stacking, the AA stacked bilayer graphene retains gapless in the presence of an applied field.[58] Thus, both the AAA- and ABA-stacked graphene/BN/graphene trilayers would behave like an AB-stacked graphene bilayer.

The asymmetry induced by the central BN layer breaks the band degeneracy between the two carbon sublattices within each graphene layer. On the other hand, degeneracy between the top and bottom graphene layers is lifted when we apply the electric field. Therefore, asymmetry between two sublattices within each graphene layer and asymmetry between the top and bottom graphene layers leads to a finite energy gap in the trilayer system.

In the ABC stacking, no carbon atoms of the top graphene can interact with the bottom layer *via* BN (Fig. 1), so the coupling between graphene layers in this configuration is weakest. Note the 'Mexican hat' pattern in band structures shown in Fig. 5 is the signature of biased coupled graphene bilayer, where the magnitude of the minimal energy gap reflects the coupling strength between two graphene layers. Thus we argue that the AAA and ABA stacked graphene/BN/graphene trilayers just behave like graphene bilayers but with weaker coupling, while ABC stacked graphene/BN/graphene trilayer behaves like two uncoupled graphene monolayers when an electric field is applied. For the case of trilayer graphene, on the other hand, it has been argued that the loss of mirror symmetry in the ABC-stacked trilayer introduces asymmetry in the sublattices, which is enhanced by the external electric field compared to the cases of AAA- or ABA-stacked configurations.[44,59]

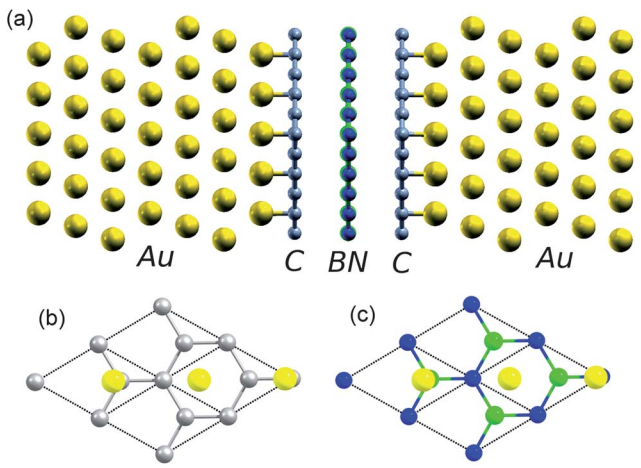

Fig. 6 (a) A side view of the ABA stacked graphene/BN/graphene trilayer coupled with semi-infinite bulk gold contacts. (b) Contact detail between gold and graphene in panel (a). (c) Contact detail between gold and BN in a BN/graphene/BN transport calculation. Symbols: C in grey, B in green, N in blue and Au in yellow.

Electronic transport properties

The contact leads for transport calculations are composed of semi-infinite Au-(111) surfaces which are comprised of 6 (top) and 7 (bottom) atomic layers. For trilayers, the distance between gold and the nearest monolayer is taken to be 2.1 Å, while the distance between the left and the right gold electrodes is 11 Å. The Mullikan population analysis suggests that no charge transfer takes place between Au atoms and graphene or BN monolayers, though a relatively strong interaction exists between gold and the monolayers in this device configuration. For example, the average valence charge of carbon atoms in the gold–(ABA) graphene/BN/graphene–gold configuration is 4.0045 e^{-}.

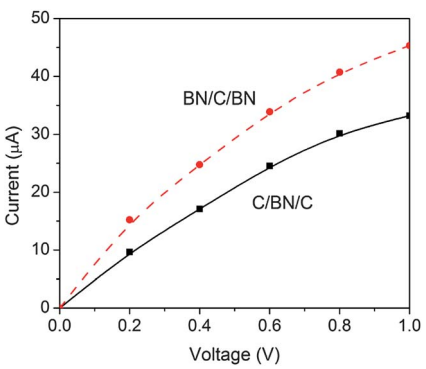

Fig. 7 The *I*–*V* characteristics of the ABA-stacked graphene/BN/graphene and ABA-stacked BN/graphene/BN trilayers coupled with gold contacts (see, Fig. 6).

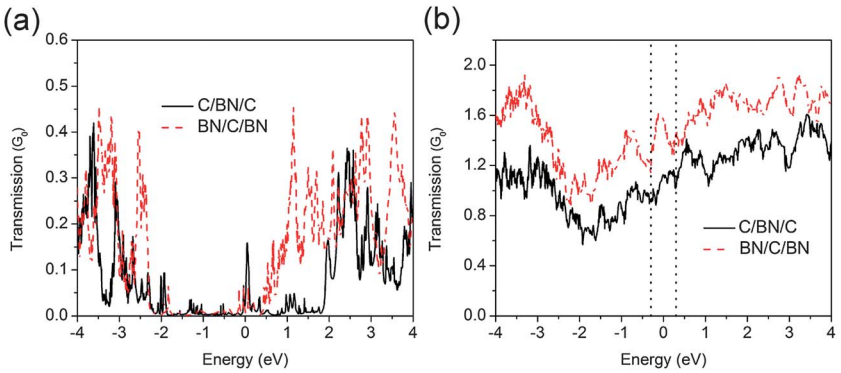

Fig. 8 Transmission function as a function of energy of ABA-stacked graphene/BN/graphene and ABA-stacked BN/graphene/BN trilayers: (a) bias = 0 (b) bias = 0.6 V. Zero of the energy is aligned to the Fermi level.

Note that the lattice mismatch between the Au-(111) surface and graphene is about 1.5%. Such a device configuration (Fig. 6) has been commonly used in previous theoretical studies investigating interactions between graphene and metallic systems.[42,44,53]

The calculated *I–V* characteristics of the ABA-stacked trilayers for the perpendicular applied bias are shown in Fig. 7. The results show a nearly metal-like conduction for both graphene/BN/graphene and BN/graphene/BN in the low-field regime. This is consistent with zero-field transmission functions of these configurations as shown in Fig. 8(a). It is clear from the figure that both graphene/BN/graphene and BN/graphene/BN trilayers have a non-negligible transmission at the Fermi energy. With increase in the bias voltage, both graphene/BN/graphene and BN/graphene/BN trilayers exhibit a low-gap, p-type semiconducting behavior. Interestingly, the zero-field gap-opening in BN/graphene/BN does not appear to suppress the current. In fact, the magnitude of the calculated current is even slightly higher than that in the case of graphene/BN/graphene at a given applied bias voltage. We attribute this to the difference in the effect of the external electric field on the band gap of the two systems – a nearly field-independent band gap of the BN/graphene/BN trilayer *versus* a variable band gap of the graphene/BN/graphene system. Additionally, the difference in the nature of chemical bonding at the Au–graphene and Au–BN interfaces, as shown in Fig. 9, also contributes to a higher current in the Au–BN/graphene/BN–Au system than in the Au–graphene/BN/graphene–Au.

There exists a relatively strong bonding between gold and boron/nitrogen atoms of BN relative to gold and carbon atoms (Fig. 9) which provides additional conduction channels for BN/graphene/BN. This is confirmed by the presence of additional conduction band-derived states in the finite field transmission function of BN/graphene/BN shown in Fig. 8 considering that the transmission function, in general, reflects the intrinsic transmission characteristics of the trilayer system.

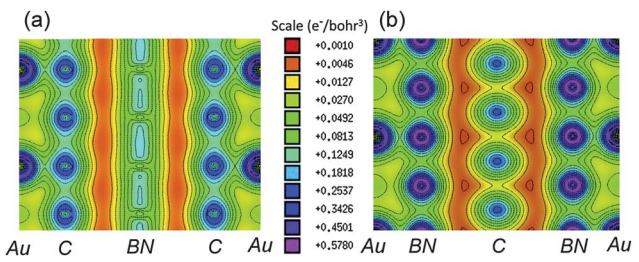

Fig. 9 The valence charge density contours of (a) ABA-stacked graphene/BN/graphene, and (b) ABA-stacked BN/graphene/BN trilayers coupled with gold contacts.

IV. Conclusion

Electronic structure calculations at the level of vdW-DFT theory together with non-equilibrium Green's Function method were performed on mixed trilayers composed of graphene and BN. These trilayers exhibit strong stacking dependence on the interlayer interactions and the electronic band structure. The binding energy for the graphene/BN/graphene system shows the order ABA > ABC > AAA whereas the order is ABC ~ ABA > AAA for BN/graphene/BN trilayer. In both cases, AAA stacking yields significantly lower binding energies than that for ABA or ABC stacking. The graphene/BN/graphene trilayer shows almost zero (~1 meV) gap in the band structure at *K* point for ABA stacking and very small, 4 meV and 6 meV, gap for the AAA and ABC stacking configurations, respectively. The BN/graphene/BN trilayer, on the other hand, shows a finite band gap that depends on the stacking arrangement in the order: AAA > ABA > ABC.

The presence of an external electric field applied perpendicular to the planes of the trilayers shows remarkable differences in the tunability of the band gap of the two cases. Whereas the zero-field band gap in the case of BN/graphene/BN trilayer remains unaffected by the external field, the graphene/BN/graphene trilayer in its AAA and ABA stacking configurations exhibit spectacular tunability in the low field (*i.e.*, below 0.5 V nm^{-1}) regime. The calculations reveal that in the low-field regime, both graphene/BN/graphene and BN/graphene/BN show a metal-like conduction that change to a low-gap semiconductor, with p-type *I–V* characteristics.

Pristine graphene as a genuine 2D material shows a variety of extraordinary properties. Nevertheless, graphene has its own limitations. For example, absence of a finite energy gap hampers graphene from functioning as practical electronic devices.[57] On the other hand, it has been shown that application of an electric field is required to induce a finite gap in the graphene layers (*e.g.*, graphene bilayer[57] and ABC stacked trilayer system[23,24,27,59]). In our case, the proposed graphene/BN/graphene trilayer system offers an alternative way to induce the gap with different

saturation values of the electric field which is distinct from what is observed for the graphene layer systems.

Direct growth of graphene on h-BN and *vice versa* has been achieved by CVD methods.[19,20,60] These experimental results have paved the way for realizing high-quality graphene/BN hybrid layered structures. The proposed trilayer structure can be fabricated using two CVD steps: fabrication of a graphene/BN bilayer followed by a deposition of graphene forming a trilayer system. Since thicker layers of two-dimensional sheets of graphene, BN and their hybrid structures are more easily accessible in the experiments, both graphene/BN/graphene and BN/graphene/BN graphene trilayers can be useful for applications in nanoscale devices, as the present study shows.

Acknowledgements

Helpful discussions with Saikat Mukhopadhyay, S. Gowtham and Dongwei Xu are acknowledged. The work at Michigan Technological University was performed under support by the Army Research Office through Contract Number W911NF-09-1-0221. RHS acknowledges the support of the Swedish Research Council (VR, grant no. 621-2009-3628).

References

1 N. Savage, Materials science: super carbon, *Nature*, 2012, **483**, S30–S31.
2 K. Bourzac, Electronics: back to analogue, *Nature*, 2012, **483**, S34–S36.
3 A. H. Castro Neto, F. Guinea, N. M. R. Peres, K. S. Novoselov and A. K. Geim, The electronic properties of graphene, *Rev. Mod. Phys.*, 2009, **81**, 109.
4 J. Park, W. C. Mitchel, G. J. Brown, S. Elhamri, L. Grazulis, H. E. Smith, S. D. Pacley, J. J. Boeckl, K. G. Eyink, S. Mou, D. H. Tomich and J. E. Hoelscher, Band gap formation in graphene by *in situ* doping, *Appl. Phys. Lett.*, 2011, **98**, 203102.
5 P. P. Shinde and V. Kumar, Direct band gap opening in graphene by BN doping: *ab initio* calculations, *Phys. Rev. B: Condens. Matter Mater. Phys.*, 2011, **84**, 125401.
6 N. Gorjizadeh and Y. Kawazoe, Chemical functionalization of graphene nanoribbons, *J. Nanomater.*, 2010, 513501.
7 S. Y. Zhou, G. H. Gweon, A. V. Fedorov, P. N. First, W. A. de Heer, D. H. Lee, F. Guinea, A. H. Castro Neto and A. Lanzara, Substrate-induced bandgap opening in epitaxial graphene, *Nat. Mater.*, 2007, **6**, 770–775.
8 Y.-J. Kang, J. Kang and K. J. Chang, Electronic structure of graphene and doping effect on SiO_2, *Phys. Rev. B: Condens. Matter Mater. Phys.*, 2008, **78**, 115404.
9 G. Giovannetti, P. A. Khomyakov, G. Brocks, P. J. Kelly and J. van den Brink, Substrate-induced band gap in graphene on hexagonal boron nitride: *ab initio* density functional calculations, *Phys. Rev. B: Condens. Matter Mater. Phys.*, 2007, **76**, 073103.
10 F. Xia, D. B. Farmer, Y.-m. Lin and P. Avouris, Graphene field-effect transistors with high on/off current ratio and large transport band gap at room temperature, *Nano Lett.*, 2010, **10**, 715–718.
11 R. Balu, X. Zhong, R. Pandey and S. P. Karna, Effect of electric field on the band structure of graphene/boron nitride and boron nitride/boron nitride bilayers, *Appl. Phys. Lett.*, 2012, **100**, 052104.
12 X. Zhong, Y. K. Yap, R. Pandey and S. P. Karna, First-principles study of strain-induced modulation of energy gaps of graphene/BN and BN bilayers, *Phys. Rev. B: Condens. Matter Mater. Phys.*, 2011, **83**, 193403.
13 A. Ramasubramaniam, D. Naveh and E. Towe, Tunable band gaps in bilayer graphene–BN heterostructures, *Nano Lett.*, 2011, **11**, 1070–1075.
14 J. Sławińska, I. Zasada and Z. Klusek, Energy gap tuning in graphene on hexagonal boron nitride bilayer system, *Phys. Rev. B: Condens. Matter Mater. Phys.*, 2010, **81**, 155433.
15 C. R. Dean, A. F. Young, I. Meric, C. Lee, L. Wang, S. Sorgenfrei, K. Watanabe, T. Taniguchi, P. Kim, K. L. Shepard and J. Hone, Boron nitride substrates for high-quality graphene electronics, *Nat. Nanotechnol.*, 2010, **5**, 722–726.
16 J. Xue, J. Sanchez-Yamagishi, D. Bulmash, P. Jacquod, A. Deshpande, K. Watanabe, T. Taniguchi, P. Jarillo-Herrero and B. J. LeRoy, Scanning tunnelling microscopy and spectroscopy of ultra-flat graphene on hexagonal boron nitride, *Nat. Mater.*, 2011, **10**, 282–285.
17 B. Sachs, T. O. Wehling, M. I. Katsnelson and A. I. Lichtenstein, Adhesion and electronic structure of graphene on hexagonal boron nitride substrates, *Phys. Rev. B: Condens. Matter Mater. Phys.*, 2011, **84**, 195414.
18 Y. Sakai, T. Koretsune and S. Saito, Electronicstructure and stability of layered superlattice composed of graphene and boron nitride monolayer, *Phys. Rev. B: Condens. Matter Mater. Phys.*, 2011, **83**, 205434.
19 Z. Liu, L. Song, S. Zhao, J. Huang, L. Ma, J. Zhang, J. Lou and P. M. Ajayan, Direct growth of graphene/hexagonal boron nitride stacked layers, *Nano Lett.*, 2011, **11**, 2032–2037.
20 S. Tang, G. Ding, X. Xie, J. Chen, C. Wang, X. Ding, F. Huang, W. Lu and M. Jiang, Nucleation and growth of single crystal graphene on hexagonal boron nitride, *Carbon*, 2012, **50**, 329–331.
21 L. Britnell, R. V. Gorbachev, R. Jalil, B. D. Belle, F. Schedin, A. Mishchenko, T. Georgiou, M. I. Katsnelson, L. Eaves, S. V. Morozov, N. M. R. Peres, J. Leist, A. K. Geim, K. S. Novoselov and L. A. Ponomarenko, Field-effect tunneling transistor based on vertical graphene heterostructures, *Science*, 2012, **335**, 947–950.
22 J. E. Padilha, R. B. Pontes and A. Fazzio, Bilayer graphene on h-BN substrate: investigating the breakdown voltage and tuning the bandgap by electric field, *J. Phys.: Condens. Matter*, 2012, **24**, 075301.
23 C. H. Lui, Z. Li, K. F. Mak, E. Cappelluti and T. F. Heinz, Observation of an electrically tunable band gap in trilayer graphene, *Nat. Phys.*, 2011, **7**, 944–947.
24 W. Bao, L. Jing, J. Velasco, Y. Lee, G. Liu, D. Tran, B. Standley, M. Aykol, S. B. Cronin, D. Smirnov, M. Koshino, E. McCann, M. Bockrath and C. N. Lau, Stacking-dependent band gap and quantum transport in trilayer graphene, *Nat. Phys.*, 2011, **7**, 948–952.
25 K. Tang, R. Qin, J. Zhou, H. Qu, J. Zheng, R. Fei, H. Li, Q. Zheng, Z. Gao and J. Lu, Electric-field-induced energy gap in few-layer graphene, *J. Phys. Chem. C*, 2011, **115**, 9458–9464.
26 F. Zhang, J. Jung, G. A. Fiete, Q. Niu and A. H. MacDonald, Spontaneous quantum hall states in chirally stacked few-layer graphene systems, *Phys. Rev. Lett.*, 2011, **106**, 156801.
27 F. Zhang, B. Sahu, H. Min and A. H. MacDonald, Band structure of ABC-stacked graphene trilayers, *Phys. Rev. B: Condens. Matter Mater. Phys.*, 2010, **82**, 035409.
28 J. Sławińska, I. Zasada, P. Kosiński and Z. Klusek, Reversible modifications of linear dispersion: graphene between boron nitride monolayers, *Phys. Rev. B: Condens. Matter Mater. Phys.*, 2010, **82**, 085431.
29 R. Quhe, J. Zheng, G. Luo, Q. Liu, R. Qin, J. Zhou, D. Yu, S. Nagase, W.-N. Mei, Z. Gao and J. Lu, Tunable and sizable band gap of single-layer graphene sandwiched between hexagonal boron nitride, *NPG Asia Mater.*, 2012, **4**, e6.
30 G. Román-Pérez and J. M. Soler, Efficient implementation of a van der Waals density functional: application to double-wall carbon nanotubes, *Phys. Rev. Lett.*, 2009, **103**, 096102.
31 D. SanchezPortal, P. Ordejon, E. Artacho and J. M. Soler, Density-functional method for very large systems with LCAO basis sets, *Int. J. Quantum Chem.*, 1997, **65**, 453–461.
32 M. Dion, H. Rydberg, E. Schröder, D. C. Langreth and B. I. Lundqvist, van der Waals density functional for general geometries, *Phys. Rev. Lett.*, 2004, **92**, 246401.
33 D. C. Langreth, *et al.*, A density functional for sparse matter, *J. Phys.: Condens. Matter*, 2009, **21**, 084203.
34 J. Kleis, E. Schröder and P. Hyldgaard, Nature and strength of bonding in a crystal of semiconducting nanotubes: van der Waals density functional calculations and analytical results, *Phys. Rev. B: Condens. Matter Mater. Phys.*, 2008, **77**, 205422.
35 N. Troullier and J. L. Martins, Efficient pseudopotentials for plane-wave calculations, *Phys. Rev. B: Condens. Matter*, 1991, **43**, 1993.

36 G. Gui, J. Li and J. Zhong, Band structure engineering of graphene by strain: first-principles calculations, *Phys. Rev. B: Condens. Matter Mater. Phys.*, 2008, **78**, 075435.
37 V. M. Pereira, A. H. Castro Neto and N. M. R. Peres, Tight-binding approach to uniaxial strain in graphene, *Phys. Rev. B: Condens. Matter Mater. Phys.*, 2009, **80**, 045401.
38 R. M. Ribeiro, V. M. Pereira, N. M. R. Peres, P. R. Briddon and A. H. C. Neto, Strained graphene: tight-binding and density functional calculations, *New J. Phys.*, 2009, **11**, 115002.
39 M. Brandbyge, J. L. Mozos, P. Ordejón, J. Taylor and K. Stokbro, Density-functional method for nonequilibrium electron transport, *Phys. Rev. B: Condens. Matter Mater. Phys.*, 2002, **65**, 165401.
40 X. Zhong, R. Pandey, A. R. Rocha and S. P. Karna, Can single-atom change affect electron transport properties of molecular nanostructures such as C60 fullerene?, *J. Phys. Chem. Lett.*, 2010, **1**, 1584–1589.
41 X. Zhong, R. Pandey and S. P. Karna, Stacking dependent electronic structure and transport in bilayer graphene nanoribbons, *Carbon*, 2012, **50**, 784–790.
42 G. Giovannetti, P. A. Khomyakov, G. Brocks, V. M. Karpan, J. van den Brink and P. J. Kelly, Doping graphene with metal contacts, *Phys. Rev. Lett.*, 2008, **101**, 026803.
43 M. Vanin, J. J. Mortensen, A. K. Kelkkanen, J. M. Garcia-Lastra, K. S. Thygesen and K. W. Jacobsen, Graphene on metals: a van der Waals density functional study, *Phys. Rev. B: Condens. Matter Mater. Phys.*, 2010, **81**, 081408.
44 I. Hamada and M. Otani, Comparative van der Waals density-functional study of graphene on metal surfaces, *Phys. Rev. B: Condens. Matter Mater. Phys.*, 2010, **82**, 153412.
45 R. Laskowski, P. Blaha and K. Schwarz, Bonding of hexagonal BN to transition metal surfaces: an *ab initio* density-functional theory study, *Phys. Rev. B: Condens. Matter Mater. Phys.*, 2008, **78**, 045409.
46 S. K. Saha, U. V. Waghmare, H. R. Krishnamurthy and A. K. Sood, Phonons in few-layer graphene and interplanar interaction: a first-principles study, *Phys. Rev. B: Condens. Matter Mater. Phys.*, 2008, **78**, 165421.
47 S. B. Trickey, F. Müller-Plathe, G. H. F. Diercksen and J. C. Boettger, Interplanar binding and lattice relaxation in a graphite dilayer, *Phys. Rev. B: Condens. Matter*, 1992, **45**, 4460.
48 J. Li, G. Gui and J. Zhong, Tunable bandgap structures of two-dimensional boron nitride, *J. Appl. Phys.*, 2008, **104**, 094311.
49 R. Zacharia, H. Ulbricht and T. Hertel, Interlayer cohesive energy of graphite from thermal desorption of polyaromatic hydrocarbons, *Phys. Rev. B: Condens. Matter Mater. Phys.*, 2004, **69**, 155406.
50 L. X. Benedict, N. G. Chopra, M. L. Cohen, A. Zettl, S. G. Louie and V. H. Crespi, Microscopic determination of the interlayer binding energy in graphite, *Chem. Phys. Lett.*, 1998, **286**, 490–496.
51 D. Stradi, S. Barja, C. Díaz, M. Garnica, B. Borca, J. J. Hinarejos, D. Sánchez-Portal, M. Alcamí, A. Arnau, A. L. Vázquez de Parga, R. Miranda and F. Martín, Role of dispersion forces in the structure of graphene monolayers on Ru surfaces, *Phys. Rev. Lett.*, 2011, **106**, 186102.
52 C. Busse, P. Lazić, R. Djemour, J. Coraux, T. Gerber, N. Atodiresei, V. Caciuc, R. Brako, A. T. N'Diaye, S. Blügel, J. Zegenhagen and T. Michely, Graphene on Ir(111): physisorption with chemical modulation, *Phys. Rev. Lett.*, 2011, **107**, 036101.
53 J. Slstrokawinacuteska, P. Dabrowski and I. Zasada, Doping of graphene by a Au(111) substrate: calculation strategy within the local density approximation and a semiempirical van der Waals approach, *Phys. Rev. B: Condens. Matter Mater. Phys.*, 2011, **83**, 245429.
54 K. Müller-Dethlefs and P. Hobza, Noncovalent interactions: a challenge for experiment and theory, *Chem. Rev.*, 1999, **100**, 143–168.
55 X. Zhong, R. Pandey and S. P. Karna, The band gap tunability of AAA, ABA and ABC stacked graphene trilayers, 2012, unpublished.
56 O. Hod, Graphite and hexagonal boron-nitride have the same interlayer distance. Why?, *J. Chem. Theory Comput.*, 2012, **8**, 1360–1369.
57 Y. Zhang, T.-T. Tang, C. Girit, Z. Hao, M. C. Martin, A. Zettl, M. F. Crommie, Y. R. Shen and F. Wang, Direct observation of a widely tunable bandgap in bilayer graphene, *Nature*, 2009, **459**, 820–823.
58 J. R. Huang, J. Y. Lin, B. H. Chen and M. H. Tsai, Structural and electronic properties of few-layer graphenes from first-principles, *Phys. Status Solidi B*, 2008, **245**, 136–141.
59 B.-R. Wu, Field modulation of the electronic structure of trilayer graphene, *Appl. Phys. Lett.*, 2011, **98**, 263107.
60 M. Son, H. Lim, M. Hong and H. C. Chio, Direct growth of graphene pad on exfoliated hexagonal boron nitride surface, *Nanoscale*, 2011, **3**, 3089–3093.

